Strojniški vestnik - Journal of Mechanical Engineering 53(2007)7-8, 491-502
UDK - UDC 678.056:678.7
Izvirni znanstveni članek - Original scientific paper (1.01)

Ocena tlaka v kalupu za stroškovni model obstojnosti stroja za batno brizganje

Cavity-Pressure Estimation for a Piston-Moulding Life-Cycle Cost Model

Charl L. Goussard - Anton H. Basson
(Stellenbosch University, South Africa)

Pričujoči prispevek predstavlja in vrednoti postopek za hitro oceno tlakov v kalupu med batnim brizganjem termoplastičnih materialov. Postopek uvaja analitične rešitve v manjšem številu nadzornih prostornin. Rezultat je delno analitičen model, namenjen uporabi med optimizacijo konstrukcije strojev za batno brizganje, kar vodi do optimizacije stroškov v celotnem krogu obstojnosti izdelka. Model je prav tako mogoče prilagoditi primerom brizganja. S tem namenom so pojasnjene tudi nekatere prednosti in pomanjkljivosti batnega brizganja v primerjavi z injekcijskim. Glavna prednost delno analitičnega modela je hitrost, s katero je določena razmeroma točna ocena tlaka brizganja v kalup. Tak pristop pride še posebej v poštev, kadar bi bile numerične simulacije preobsežne in časovno potratne, na primer v primerih optimizacij s širokim razponom neodvisnih spremenljivk. Prav tako so obravnavani različni analitični tokovni modeli, ki jih je moč najti v literaturi, ter njihova možnost uporabe v področju injekcijskega brizganja. Sledi obravnava izpeljanega delno analitičnega modela z njegovimi pripadajočimi poenostavitvami. Njegovi rezultati so primerjani z numeričnimi rešitvami na treh primerih. Ti primeri so pokazali, da je model dovolj natančen za zasnovo konstrukcije naprave in za raziskave stroškovnih usmeritev obstojnosti naprave.

(Ključne besede: brizganje polimerov, batno brizganje, tlaki v kalupu, optimiranje stroškov)

In this paper we propose and evaluate an approach for quickly estimating the cavity pressures during the piston moulding of thermoplastics. The approach applies analytical solutions in a small number of control volumes. The resulting semi-analytical model is intended for use when optimising the design of piston moulding machines, leading to a life-cycle cost optimisation. The model is also applicable to similar injection-moulding cases. Some advantages and disadvantages of piston moulding, compared to injection moulding, are discussed. The main contribution of the semi-analytical model is the speed with which a reasonably accurate estimate of the cavity injection pressure is calculated. This approach is useful in cases when numerical simulations would be too cumbersome and time consuming, e.g., in optimisation studies where the independent variables could vary over a wide range. Different analytical flow models found in the literature and their applicability to injection moulding are discussed. This is followed by a discussion of the derived semi-analytical model, with its underlying simplifications. The results from the semi-analytical model are compared to numerical solutions for three case studies. These case studies show that the model is sufficiently accurate for machine-layout design purposes and for investigating life-cycle cost trends.

(Keywords: injection moulding, piston moulding, cavity pressure, cost modelling)

0 INTRODUCTION

Lomolding is a piston moulding process designed to make similar parts to injection moulding. Its main operational sequence (illustrated in Fig. 1) starts by measuring off in the metering cylinder the exact amount of molten thermoplastic required for a part, transferring the melt to the moulding cylinder and then pushing the melt into the moulding cavity with the moulding piston. During solidification, the moulding piston holds the cavity under pressure and the piston face forms part of the cavity wall.

The area where the melt enters the cavity is much larger than the typical sprue of injection moulding, which is anticipated to bring advantages,

such as the ability to mould long fibres, lower material shear rates, and lower clamping-force requirements.

A life-cycle cost model is being developed to optimise the designs of the lomolding machine and to investigate the range of products suitable for the profitable application of lomolding. This model is aimed at the part of the life-cycle cost of a lomolded product that is related to the processing (as opposed to that contributed by the material used, the distribution, disposal, etc). The processing's contribution to the life-cycle cost is largely determined by the design of the lomolding machine and the processing parameters. Typical issues that must be addressed, considering the life-cycle cost and the quality of a part, are the optimum ratio of the moulding-piston area to the part projected area, the choice between electric and hydraulic actuators, and the choice between a single piston and multiple piston arrays. The effect of design and process choices on the energy consumption must also be assessed.

These machine-design and processing parameters are strongly driven by the injection pressure needed to fill a mould cavity, as well as the clamping force needed to resist the cavity pressures to avoid material flashing. To investigate the processing's contribution to the life-cycle costs and to optimise the design for minimum cost, a method is therefore needed to quickly obtain the injection pressure and clamp force needed to produce a certain part for a range of operating parameters (i.e., cycle time, melt and mould temperatures, and material properties). As little as possible user intervention should be required in the early design phases to facilitate the automation of the optimisation process, but the dominant physical aspects, such as the effect of fill rate, solidification rate against the mould walls during mould filling, and the non-Newtonian character of the flow, must be accounted for.

In practice, numerical simulation programs (Cadmould, Mouldflow, etc.) are used to analyse the behaviour of the molten material before expensive moulds are manufactured. These programs require a large amount of user interaction (creating a mesh, setting large numbers of process and material parameters, cumbersome post-processing, etc.) to accurately simulate a specific part and are therefore not suitable for the cost modelling required to explore the overall machine-design decisions and optimisation. Numerical methods can, however, be used to obtain more accurate pressure predictions once the solution region is narrowed down with the use of other methods. This approach can be used when similar trends are predicted by the approximate and the more accurate methods.

Analytical solutions for non-Newtonian flow with solidification in simple geometries have been reported, e.g., the flow between parallel plates, the flow in round tubes and disc flow geometries (outlined in Section 3). Since the analytical solutions are only applicable to a limited range of geometries, they cannot be applied as such in the cost model. The approach described in the present paper is to subdivide the cavity into a small number of simple, large control volumes and to use the

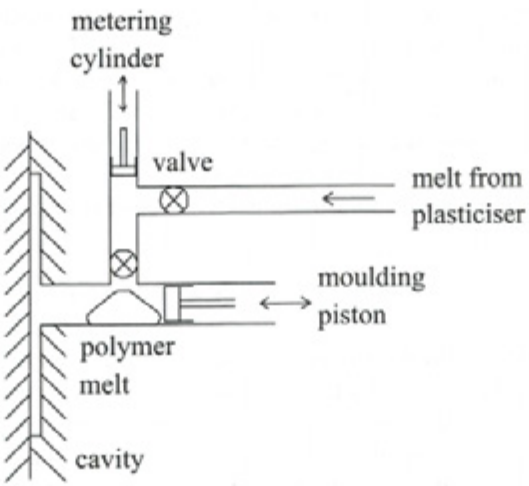

Fig. 1. *The lomolding process*

analytical solutions to approximate the flow in each control volume. The key factors in the success of the approach are formulating an equivalent flow pattern in each control volume and selecting the appropriate analytical solution for that control volume, such that the prediction of the solidification rate gives the correct overall results. Once the effective flow areas (h^*) are known, the pressure profiles can be calculated fairly easily.

The work presented in this paper was driven by the development of lomolding. However, most of the results are equally applicable to injection moulding. The paper's main contribution is an approach to reasonably accurately estimate the cavity pressures during mould filling, which is fast and simple enough to use for optimisation studies.

1 LITERATURE REVIEW

Researchers have shown an interest in theoretical and experimental studies involving fluid flow with solidification in circular tubes and on the walls of parallel-plate channels. The effect of this solidification layer on laminar flow heat transfer has been reported ([1] to [3]). Zerkle and Sunderland [1] and Lee and Zerkle [4] studied the steady solidification of fluid flow for Newtonian fluids with constant physical properties and no viscous heating. They cast the energy equation into a form which is similar to one that describes the classical Graetz problem. The solution is found by the method of the separation of variables and it takes the form of an infinite sum of eigenvalues.

Janeschitz-Kriegl [5] and Dietz et al. [6] proposed methods to calculate the thickness of the frozen layer that is formed on the cold cavity walls during the injection-moulding process. Janeschitz-Kriegl [5] used a steady-state heat-transfer coefficient, and the viscous heat generated was estimated from the average melt velocity and the pressure gradient under isothermal conditions. Dietz et al. [6] estimated the thickness of the frozen solid layer by applying the solution for an infinite solid slab. Janeschitz-Kriegl [7] showed in a later paper that a more detailed study with the aid of coupled motion and energy equations will not improve the accuracy of the solid-layer thickness estimation. Effects such as the glass transition or the crystallization kinetics at extreme rates of cooling and shearing have a strong influence on these results.

Richardson et al. [8] described the benefits of decomposing moulding networks into basic geometries and solving an analytical flow problem for each segment. This scheme aided mould-maker decisions regarding hot-runner, sprue and mould design. Richardson [9] extended the solution of Zerkle and Sunderland [1] and Lee and Zerkle [4] to non-Newtonian fluids with viscous heating. Again, the energy equation is transformed and the temperature and the frozen-layer thickness are expanded in a power series. The thickness of the frozen layer is then computed by substituting the first three terms of the power series into the energy equation. This solution is well suited for material flows with high Graetz (Gz) numbers, i.e., in the thermal-entrance region. The Graetz number is the ratio between the heat convection in the flow direction and the heat conduction in the direction perpendicular to the flow. In the work presented here, the solutions for flow between parallel plates were used. These solutions and how they are adapted to compute flows in discs, for instance, are described in more detail in Section 2.

Richardson also published three papers on flows with freezing of variable-viscosity fluids. The first [10] described developing flows with very high heat generation due to viscous dissipation that is large enough to cause significant variations in viscosity. However, the difference between the polymer temperature at the inlet to a specific part of the mould network and the melting temperature of the polymer is assumed not to cause significant variations in polymer viscosity.

The second paper [11] described developing flows with very low heat generation due to viscous dissipation. Furthermore, the difference between the temperature of the polymer at the entry to a specific part of the mould network and the melting temperature of the polymer is assumed to be sufficiently large so as to cause significant variations in polymer viscosity. Polymer flows in pipes, between discs and between parallel plates were considered.

These results compare reasonably well with the results obtained from Richardson's [9] previous paper, as long as the flow Graetz number is sufficiently large. However, combining the closed-form solutions for the three different geometry types, as will be required for the work presented in this paper, is not feasible.

In the third paper, Richardson [12] discussed solutions for cases where the polymer flow is fully developed.

The first models proposed by Richardson [10] did not produce good results for typical lomolding flows when compared to numerical simulation results. It could be argued that the variations in the shear rate are overshadowed by the large difference between the polymer inlet temperature and the polymer melt temperature (± 70°C) and therefore the second paper [11] produces more acceptable results. The third paper's flow solutions are not applicable to lomolding as the flows considered in the work presented here are generally undeveloped with regard to the temperature field.

All of the above papers consider polymer injection at a constant flow rate. This constant-flow-rate phase comprises approximately the first 90% of the polymer-injection stage and is followed by polymer injection at a constant pressure. Richardson published three more case studies involving cavity filling at a constant pressure: freezing off at polymer injection gates [13], freezing off in round and flat cavities [4] and freezing off in disc cavities [15]. As cavity filling occurs at a more or less constant polymer flow rate for such a large part of the injection stage, the focus in the work presented here was placed on filling at a constant flow rate.

Hill [16] proposed solutions to find the equilibrium height of the solidified polymer layer, where the polymer temperature increases due to viscous dissipation in equilibrium with the temperature drop due to heat conduction to the cold cavity wall. However, attention was restricted to the Newtonian case, for which numerical solutions are provided as well. Neither the equilibrium nor the Newtonian-flow assumptions are reasonable for the work presented here.

Today, far more complex cavities and flow geometries can be analyzed with numerical methods. Analytical models are often used to test numerical algorithms for simple case studies. Yang et al. [17] compared the results for the steady solidification of non-Newtonian fluids flowing in round tubes. Gao et al. [18] studied the effect of variable injection speed during injection-mould filling. They also tested their numerical algorithms against simple analytical solution case studies.

The scarcity of more recent papers reporting analytical solutions is probably due to the complexity of the physics involved, limiting analytical solutions to a very few simple geometries. In recent years, however, considerable effort has been invested in developing numerical simulations, mostly using finite-element modelling, that can handle the complex geometries commonly encountered when processing plastics.

2 SEMI-ANALYTICAL MODEL

This section describes Richardson's [9] analytical model briefly as well as the adaptation of the model to flows in channels of varying width. All the equations in this section come from [9].

Fig. 2 shows a schematic of the polymer flow between parallel plates. The flow is symmetrical with respect to the centreline and therefore only half of the cavity is shown. The half-height of the cavity is given by h, and the distance between the centreline and the solidified layer, by h^*. The solution is split into two regions, a thermal-entry region and a melt-front region. The melt-front region comprises most of the total flow length in typical cases.

The pressure drop (ΔP) over the entire flow length is given by Equation 1:

$$\Delta P = \mu^* \int_0^{x_f} \left(\frac{(m+2)Q}{2wh^{*m+2}} \right)^{1/m} dx \qquad (1).$$

The half-height of the polymer melt region (h^*) is found by introducing:

$$\delta = 1 - \frac{h^*}{h} \qquad (2).$$

For the thermal-entrance region, δ is given by:

$$\delta = 6\theta^* \Gamma(4/3) \left(\frac{\varepsilon}{6(m+2)Gz} \right)^{\frac{1}{3}} + 0\left(Gz^{\frac{-2}{3}} \right) \qquad (3)$$

and for the melt-front region, by:

$$\delta = 4w^* \left(\frac{\varepsilon_f - \varepsilon}{Gz} \right)^{\frac{1}{2}} \qquad (4),$$

where:

$$\theta^* = \frac{k_S (T_m - T_w)}{k_L (T_i - T_m)} \qquad (5)$$

$$\Gamma(4/3) = 0.893 \qquad (6)$$

$$\varepsilon = \frac{x}{L} \qquad (7)$$

$$\varepsilon_f = \frac{x_f}{L} \qquad (8)$$

$$\omega^* = (S_f / 2\kappa)^{0.5} \qquad (9)$$

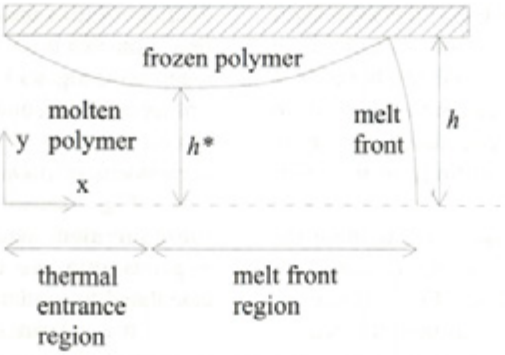

Fig. 2. *Polymer flow in a channel*

$$\kappa = \frac{k_L/(\rho_L c_L)}{k_S/(\rho_S c_S)} \quad (10).$$

The Stefan number (S_j) is the ratio of the heat required to raise the polymer temperature from the cavity wall temperature to the polymer melting point, and the heat required to melt the polymer solid.

Once the half-height of the polymer-melt region is found for a control volume, the pressure drop can be calculated. These equations were derived for cases where the flow-channel width remains constant and the flow front enters the cavity evenly over the whole channel width.

Consider a typical moulding case: a rectangular cavity with constant thickness is filled through a sprue in the centre of the cavity. Fig. 3 shows a quarter of such a cavity.

Clearly, the longest flow path is given by the diagonal line D running from the injection point to one corner. This longest flow path is divided into a number of control volumes. To calculate h^* for a specific control volume at a certain time, it is necessary to know the flow-front position along D, the start point of the control volume with respect to D, the length of this control volume along D and the average width of the control volume.

To place a particular control volume at an equivalent x-position in the analytic model, assumptions have to be made about the upstream and downstream conditions:

- The upstream flow-path length in the semi-analytical model is taken to be the same as the true (geometric) length.
- The upstream and downstream flow-path width is taken to be equal to the average width of the control volume under consideration.
- Once the melt front has passed through the control volume, its position is calculated using the above flow-channel width (even though this will, in general, not coincide with the true flow-front position).

Case studies, as shown here, have confirmed that the approximated upstream geometry gives reasonable results, even though any upstream variation in flow area will influence the time that the flow front takes to reach a control volume. The approximated downstream geometry can deviate from the true geometry without affecting the solidified layer thickness in the control volume under consideration since, for these cases where the flow rate is constant, the only upstream effect is in the pressure gradient.

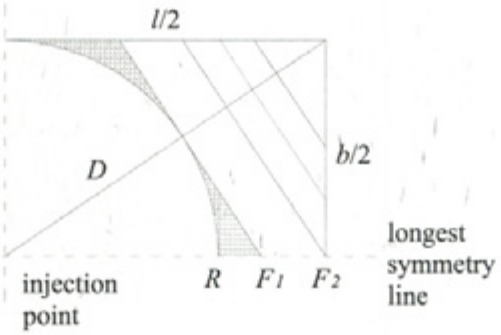

Fig. 3. *Schematic of the polymer flow front in a rectangular cavity (quarter segment shown)*

The pressure drop and the height of the solid layer are calculated for this control volume in a straightforward manner, as described above. It is necessary, in order to solve Equation 1 correctly, to check if a control volume is positioned entirely in the thermal-entrance region, entirely in the melt-front region or contains both.

Therefore, it is necessary to calculate the equivalent width, volume and start position along D for each control volume. From Fig. 3 it is clear that the flow front will be circular until the nearest side of the rectangle ($b/2$) is met. Therefore, the radius of the largest circular flow front is given by Equation 11:

$$R = \frac{b}{2} \tag{11}.$$

Up to this point, the equivalent control-volume width is given by Equation 12:

$$w_i = 2\pi R_i \tag{12}.$$

From F_1 to F_2 (Fig. 3, note F_2 is where the longest symmetry line meets the edge of the cavity) the equivalent flow widths are set equal to four times (note Fig. 3 shows a quarter of the cavity) the length of a line perpendicular to D, extending from the side of the cavity to the longest symmetry line. Note that these flow control volumes fall away when working with a square cavity (see Fig. 4). From position F_2 onwards the control-volume width is calculated as four times the length of a line perpendicular to D, extending from side to side.

Fig. 5 shows that the assumptions made for the equivalent widths of the control volumes approximate the true flow case numerically calculated by Cadmould.

It now remains to calculate the position of the melt-flow front as closely as possible to the true flow phenomenon. As is clear from Fig. 3, the hatched area is the only area not accounted for in the control volumes. To preserve the filling time, the volume associated with the hatched area is added to all the control volumes on a per-volume basis, except for the round control volumes. Once this correction has been applied, it is easy to calculate the position of the flow front.

The semi-analytical model is validated in the next section using different case studies.

3 CASE STUDIES

The semi-analytical model was implemented in software by the authors. This section shows some

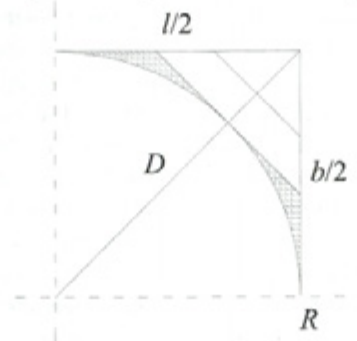

Fig. 4. *Schematic of the polymer flow front in a square cavity*

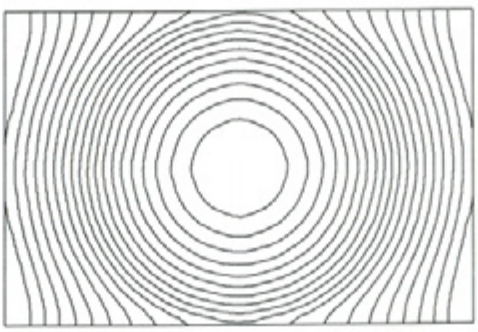

Fig. 5. *Flow lines for a rectangular cavity filled in the centre as calculated with Cadmould*

results to verify the semi-analytical model. The most restrictive requirement of the analysis presented above is that the flow Graetz number must be sufficiently high, which is explored later in this section.

The results of the semi-analytical model are compared with those of Cadmould. Although it would have been preferable to compare the results directly with experimental data, Cadmould is a widely accepted simulation tool in industry and therefore its results have considerable credibility. Furthermore, numerical simulations can give details that are extremely difficult to measure, such as the thickness of the solidified layer.

Two polymer materials suited for lomolding were selected for the case studies, i.e., Novolen 1100 N (a homogeneous polypropolene) and Celstran PP GF30 (a polypropolene with 30% glass-fibre component). The material properties for these materials given by Cadmould [19] and Osswald and Menges [20] were used and are summarised in Table 1. Cadmould [19] provides a Carreau viscosity model for these two materials. The unit shear-rate viscosity (μ^*) and the viscosity shear-rate coefficient (m) are found by fitting a power-law model to the Carreau model. The power-law viscosity model is given in Equation 13:

$$\mu = \mu^* \left| \frac{\partial u_x}{\partial y} \right|^{\frac{1}{m}-1} \qquad (13).$$

The figures in this section showing the results use the following abbreviations: AM for the semi-analytical model result; CM for the Cadmould numerical result; Cel for the Celstran material; and Nov for the Novolen material.

The first case study is the filling of a 500-mm-diameter disc, 3 mm thick, with the injection occurring along the circumference of an 80-mm-diameter piston into the cavity. Therefore, the flow-path length is shown in Fig. 6 as 210 mm. The disc is filled in one second at a constant flow rate. Fig. 6 shows that the growth of the solid layer along the flow path (a radial line) is underestimated, relative to Cadmould, for both materials. The pressure drop along the flow path relates well to the results obtained with Cadmould (Fig. 7). The lowest calculated Graetz number was 209 for the Celstran material and 230 for Novolen.

The second case study involves a square cavity with a length and breadth of 200 mm and a thickness of 2 mm. The injection point is in the centre and the longest flow path D is equal to $100\sqrt{2}$ mm. The cavity is filled in 0.5 seconds. As can be seen from Fig. 8, the semi-analytical model overestimates the growth of the solid layer in this case, especially near the end of the flow path. This leads to higher predicted pressure drops for both materials, as is clear from Fig. 9. The lowest calculated Graetz number was 134 for the Celstran material and 143 for Novolen. Note the sudden rise near the end due to the narrowing flow area.

The last case study is that of a rectangular cavity, 300 mm x 200 mm, with a thickness of 3 mm. The longest flow path D is equal to 180.28 mm. The cavity is filled in one second. Fig. 10 shows that the height of the solid layer is reasonably well predicted for both materials. As a result of this, Fig. 11 shows good agreement for the pressure drop across the rectangular cavity. The lowest calculated Graetz number was 191 for the Celstran material and 209 for Novolen.

In some situations a cavity will be filled in a time that will minimize the pressure drop experienced during filling. However, if this filling time is too long, a larger injection-pressure-capacity machine may be used, since this will save costs

Table 1. *Material properties*

Property	Novolen 1100 N	Celstran PP GF30	Unit
Unit shear-rate viscosity (μ^*)	5655	6958	N.s/m^2
Viscosity shear-rate exponent (m)	2.63	3.31	
Melt inlet temperature (T_i)	220	260	°C
Polymer melting temperature (T_m)	154	170	°C
Cavity-wall temperature (T_w)	40	55	°C
Polymer-melt thermal conductivity (k_L)	0.236	0.150	W/mK
Polymer-melt density (ρ_L)	910	994	kg/m^3
Polymer thermal diffusivity (α)	0.1043	0.0685	10^{-6} m^2/s

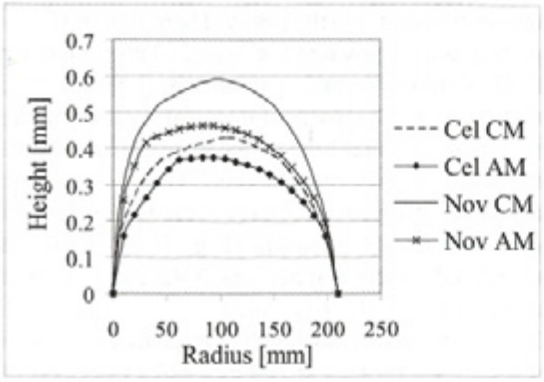

Fig. 6. *Growth of the solid layer in a disc cavity*

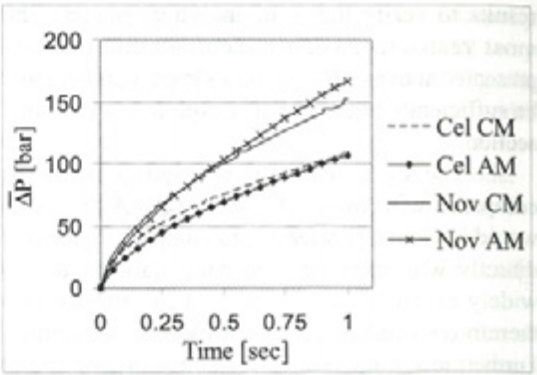

Fig. 7. *Pressure drop occurring in a disc cavity*

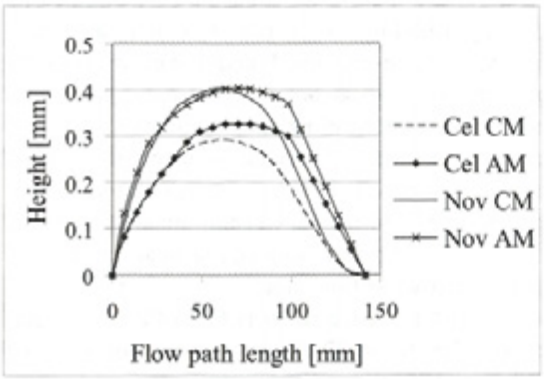

Fig. 8. *Growth of the solid layer in a square cavity*

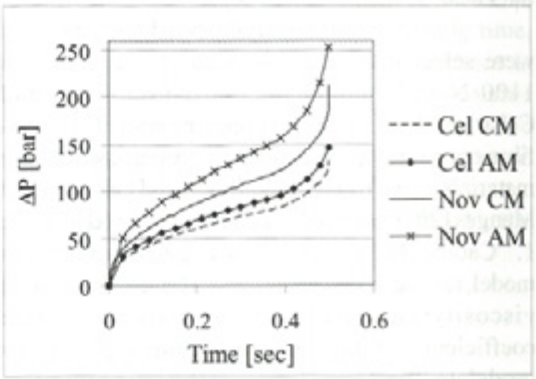

Fig. 9. *Pressure drop occurring in a square cavity*

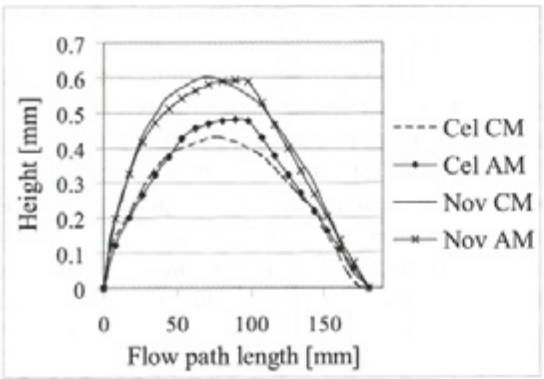

Fig. 10. *Growth of the solid layer in a rectangular cavity*

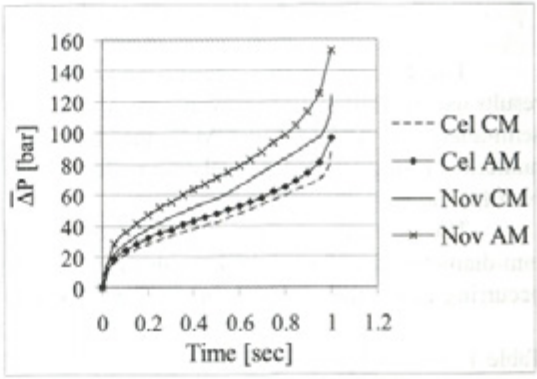

Fig. 11. *Pressure drop occurring in a rectangular cavity*

during the machine's lifetime as the part cycle time will be reduced. The fill rate directly influences the Graetz number, but the analytical model is only applicable to "large" Graetz numbers. It is therefore worth investigating what the influence is of the Graetz number on the accuracy of the semi-analytical model and what acceptable numerical values for the Graetz number would be.

Figures 12 to 15 show the influence of the Graetz number on the results obtained with the semi-analytical model for the same case studies used above. It is compared to numerical results obtained from Cadmould [19]. The Graetz numbers reported in the figures are the smallest calculated at the end of the filling stage under a constant flow rate. The objective was to find the filling time for

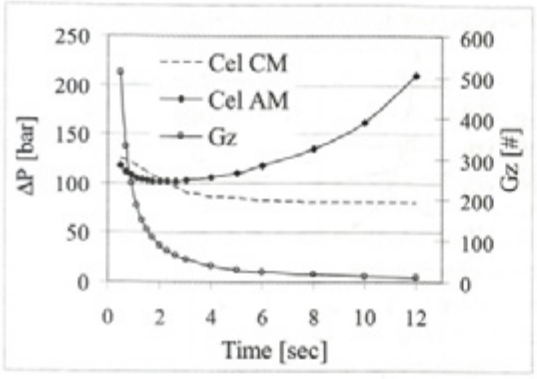

Fig. 12. *Pressure drop for different filling times in a disc cavity for Celstran material*

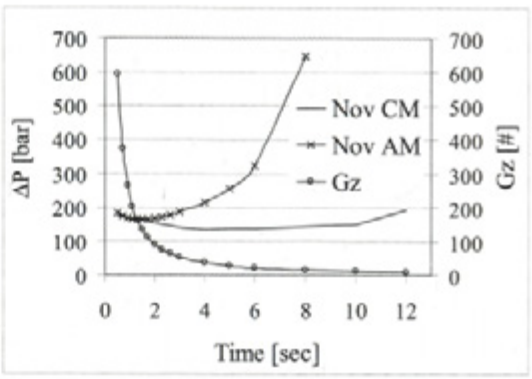

Fig. 13. *Pressure drop for different filling times in a disc cavity for Novolen material*

which the pressure drop across the cavity would be a minimum. These pressure drops are then compared to those found using the analytical model. It is also checked to see if this local minimum occurs at more or less the same filling time for both the analytical and numerical results.

Figures 12 and 13 show that for the disc cavity the pressure-drop results differ significantly for the two models when the Graetz number drops below 100. The analytical model estimates the lowest pressure drop around a 2-seconds filling time. However, Cadmould estimates these minima at around 4 seconds for both materials. At 2 seconds the error for the semi-analytical model is 6% in the case of the Novolen material and less in the case of Celstran. At 4 seconds this error grows to 59% in the worst case, which is again for the Novolen material. At this point the Graetz number is 37, well below 100.

In the case of the square cavity shown in Figures 14 and 15, the analytical model predicts the smallest pressure drop at around a filling time of 1 second for both materials. This compares well to the filling times found by Cadmould, especially in the case of the Novolen material. The minimum pressure drop varies very little across a filling time of 1 to 10 seconds in the case of the Celstran material. The error of the semi-analytical model is at most 33% for the Novolen case at a filling time of 1 second. At this point the Graetz number is equal to 57.

In the case of the rectangular cavity (Figures 16 and 17), both models predict a minimum pressure drop at around a 2-seconds cavity-fill time. In the case of the Novolen material it is noted that the analytical model calculates a slightly smaller filling time. The semi-analytical model's error is 49%, at most, for the Novolen case at a filling time of 2 seconds. At this point the Graetz number is equal to 83.

It is clear from these results that the semi-analytical model is reasonably well suited to finding

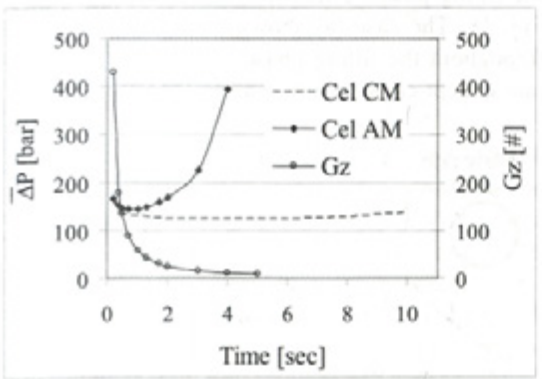

Fig. 14. *Pressure drop for different filling times in a square cavity for Celstran material*

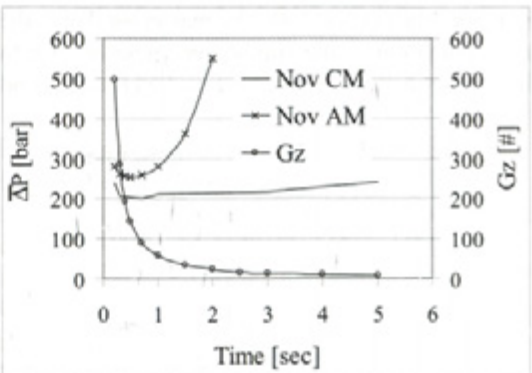

Fig. 15. *Pressure drop for different filling times in a square cavity for Novolen material*

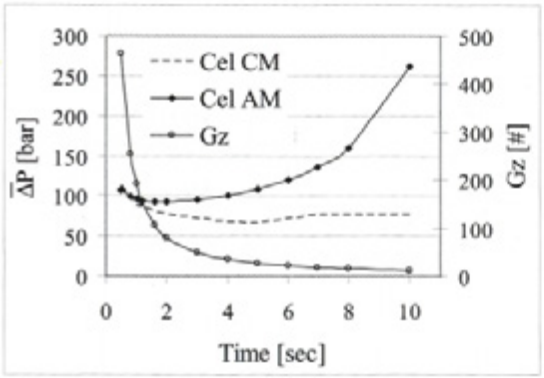

Fig. 16. *Pressure drop for different filling times in a rectangular cavity for Celstran material*

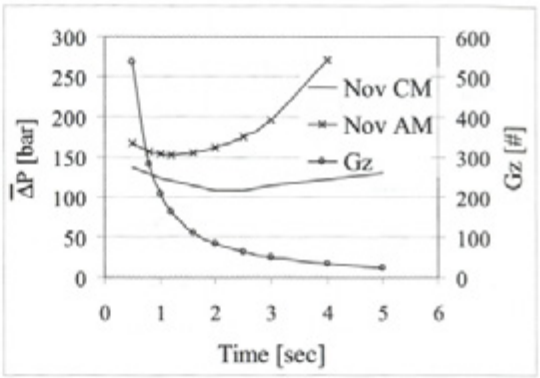

Fig. 17. *Pressure drop for different filling times in a rectangular cavity for Novolen material*

the filling time that will correspond to a minimal pressure drop across the cavity as long as the Graetz number stays above 100. Numerical simulations can then be carried out around this approximate optimum filling time and a better estimate for the pressure drop can be calculated. It is noted that the pressure drop computed by the semi-analytical model is higher than the pressure drop computed by Cadmould. This would mean that machines designed from these values will be slightly over designed and may be able to manufacture either slightly larger parts in the same time or produce the same part in a quicker cycle time.

4 CONCLUSION

The results presented above show that the semi-analytical model gives reasonable results for the pressure drop across the cavity when compared with the numerical results obtained with Cadmould. The main restriction of the model is that too high pressure drops are predicted when the Graetz number drops below 100. The reason for that is the overestimation of the solid-layer thickness due to higher conduction between the molten material and the solid layer to the cavity wall. Due to the associated smaller flow area, the overestimated solid-layer growth leads to a higher pressure drop than calculated with Cadmould. Otherwise, the model can be used for cavities with a flow-path-length to cavity-thickness aspect ratio in the range of the case studies presented here. The model provides a quick way of estimating the pressure drop across the cavity during filling, where numerical solutions would have been too cumbersome and time consuming.

The geometry-creation and computation times for the models presented here are modest to insignificant. Whether the results are accurate enough for machine-layout calculations is not easy to answer. However, the largest pressure errors occur towards the end of the filling phase. In practice a constant-pressure control strategy is used for the last part of the filling phase. The machine-sizing calculations are therefore based on the pressures encountered somewhat before the end of the filling phase. This filling method is shown in Fig. 18. The case (a) shows a constant flow rate throughout the filling phase. In case (b) the flow rate is kept constant up to a certain time and it is

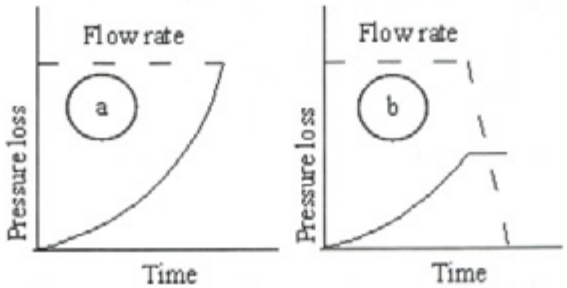

Fig. 18. *Cavity pressure loss and material flow rate during mould filling*

followed then by filling under constant pressure until the cavity is completely filled.

Since the pressures encountered during mould filling are related to the filling rate, the filling rate can in practice be reduced if the pressures exceed the design values for a given machine size. Also, the filling phase is normally much shorter than the cooling phase and the potential effects of the under/over prediction of pressure is restricted to a small part of the filling phase. Therefore, the influence of the largest pressure errors (i.e., those at the end of the filling phase) on the machine-size and cycle-time estimation is small. These pressure errors will have a small influence on the life-cycle cost, and the semi-analytical model can be expected to give useful results for machine-sizing studies and life-cycle cost assessment.

The computing times for the analytical model are insignificant on a 3-GHz computer. The computation time for the numerical results is sensitive to the finite mesh density used to model the cavities. The case studies presented here involved relatively coarse meshes to keep the computation time reasonably low, as many simulations were carried out. The computation time varied between 30 seconds and 3 minutes. The semi-analytical model will therefore yield substantially faster optimisation calculations, in addition to shorter pre- and post-processing times. Once a layout design has been selected, using the semi-analytical model presented here, final optimisation and design refinement can be done by using a numerical flow simulation package, such as Cadmould.

5 NOMENCLATURE

b	shortest side of rectangle
c_L	polymer melt specific heat capacity
c_S	frozen polymer specific heat capacity
Gz	Graetz number = $\rho_L c_L Q 2h / w k_L x$
h	half-height of cavity
h^*	half-height of the polymer-melt region
k_L	thermal conductivity of polymer melt
k_S	thermal conductivity of frozen polymer
l	longest side of rectangle
L	length of thermal entrance region
m	viscosity shear-rate coefficient
ΔP	pressure drop
Q	constant material volume flow rate
R	radius
R_i	average radius of control volume i
S_f	Stefan number = $c_S (T_m - T_w)/\Lambda$
T_i	polymer inlet melt temperature
T_m	polymer melting temperature
T_w	uniform cavity-wall temperature
u_x	polymer velocity in the flow direction
w	width of flow channel
w_i	width of flow channel of control volume i
x	axial coordinate in channel
x_f	melt-front position in channel
y	coordinate in h-direction
$\Gamma( )$	gamma function
δ	dimensionless thickness of frozen polymer
θ^*	dimensionless wall temperature
ε	dimensionless axial coordinate in channel
ε_f	dimensionless melt-front position in channel
Λ	latent heat of fusion
ρ_L	polymer melt density
ρ_S	frozen melt density
μ^*	material unit shear-rate viscosity

6 REFERENCES

[1] Zerkle, R.D., Sunderland, J.E. (1968) The effect of liquid solidification in a tube upon laminar flow heat transfer and pressure drop, *ASME Journal of Heat Transfer*, 90, pp. 183-190.

[2] Hsing-Lung, L., Hwang, G.J. (1977) An experiment on liquid solidification in thermal entrance region of a circular tube, *Letters in Heat Mass Transfer*, 4, pp. 437-444.

[3] Weigand, B., Beer, H. (1991) Heat transfer and solidification of a laminar liquid flow in a cooled parallel plate channel: The stationary case, *Wärme- und Stoffübertragung*, 19, pp. 233-240.

[4] Lee, D.G., Zerkle, R.D. (1969) The effect of liquid solidification in a parallel-plate channel upon laminar flow heat transfer and pressure drop, *ASME Journal of Heat Transfer*, 91, pp. 583-585.

[5] Janeschitz-Kriegl, H. (1977) Injection moulding of of plastics: Some ideas about the relationship between mould filling and birefringence, *Rheol. Acta*, 16, pp. 327-339.

[6] Dietz, W., White, J.L., Clark, E.S., (1978), Orientation development and relaxation in injection molding of amorphous polymers, *Polymer Engineering and Science*, 18:4, pp. 273-281.
[7] Janeschitz-Kriegl, H. (1979) Injection moulding of plastics: II. Analytical solution of heat transfer problem, *Rheol. Acta*, 18, pp. 693-701.
[8] Richardson, S.M., Pearson, H.J., Pearson, J.R.A. (1980) Simulation of injection moulding, *Plastic and Rubber: Processing*, 5, pp. 55-60.
[9] Richardson, S.M. (1983) Injection moulding of thermoplastics: Freezing during mould filling, *Rheol. Acta*, 22, pp. 223-236.
[10] Richardson, S.M. (1986a) Injection moulding of thermoplastics: Freezing of variable-viscosity fluids: Developing flows with very high heat generation, *Rheol. Acta*, 25, pp. 180-190.
[11] Richardson, S.M. (1986b) Injection moulding of thermoplastics: Freezing of variable-viscosity fluids: Developing flows with very low heat generation, *Rheol. Acta*, 25, pp. 308-318.
[12] Richardson, S.M., (1986c), Injection moulding of thermoplastics: Freezing of variable-viscosity fluids. Fully-developed flows, *Rheol. Acta*, 25, pp. 372-379.
[13] Richardson, S.M. (1985a) Injection moulding of thermoplastics. I. Freezing-off at gates, *Rheol. Acta*, 24, pp. 497-508.
[14] Richardson, S.M. (1985b) Injection moulding of thermoplastics. II. Freezing-off in cavities", *Rheol. Acta*, 24, pp. 509-518.
[15] Richardson, S.M. (1987) Freezing-off in disc cavities, *Rheol. Acta*, 26, pp. 102-105.
[16] Hill, D. (1996) Further studies of the injection moulding process, *Applied Math Modelling*, 20, pp. 719-730.
[17] Yang, L.C., Chen, S.J., Charmchi, M. (1991) Steady solidification of non-Newtonian fluid flowing in a round tube, *Polymer Engineering and Science*, 31, Nr. 3, pp. 191-196.
[18] Gao, D.M., Nguyen, K.T., Girard, P., Salloum, G. (1994) Effect of variable injection speed in injection mould filling, *Proceedings of the 52nd Annual Technical Conference*, Society of Plastic Engineers, Brookfield, CT, USA, pp. 712-715.
[19] Cadmould v6 (2002) Simcon kunststofftechnische Software GmbH, Germany, (www.simcon-worldwide.com).
[20] Osswald, T.A., Menges, G. (1995) Materials Science of Polymers for Engineers, chapters 3-4, *Hanser*, Munich, Vienna, New York.

Authors' Address: Charl L. Goussard
Prof. Dr. Anton H. Basson
Stellenbosch University
Department of Mechanical and
Mechatronic Engineering
Private Bag X1
Matieland 7602
Stellenbosch
South Africa
ahb@sun.ac.za

Prejeto: 2.5.2007
Received:
Sprejeto: 27.6.2007
Accepted:
Odprto za diskusijo: 1 leto
Open for discussion: 1 year